이학박사 학위논문

# DNA methylation이 CTCF/cohesin을 매개로 한 크로마틴의 삼차구조와 유전자 발현에 미치는 역할 규명

# Disruption of CTCF/cohesin-mediated high-order chromatin structures by DNA methylation downregulates PTGS2 expression

**2017년 8월**

서울대학교 융합과학기술대학원
분자의학 및 바이오제약학과

강지연

# DNA methylation이 CTCF/cohesin을 매개로 한 크로마틴의 삼차구조와 유전자 발현에 미치는 역할 규명

지도교수 김 태 유

이 논문을 이학박사 학위논문으로 제출함

**2017년 8월**

서울대학교 융합과학기술대학원

분자의학 및 바이오제약학과

강지연

강 지 연 의 이학박사 학위논문을 인준함

**2017년 8월**

위 원 장 _____ (인)

부위원장 _____ (인)

위 원 _____ (인)

위 원 _____ (인)

위 원 _____ (인)

# Disruption of CTCF/cohesin-mediated high-order chromatin structures by DNA methylation downregulates PTGS2 expression

by **Jee-Youn Kang**

**(Directed by Tae-You Kim, M.D., Ph.D.)**

**A thesis submitted in partial fulfillment of the requirements for the degree of Doctor of Philosophy in Department of Molecular Medicine and Biopharmaceutical Sciences at World Class University Graduate School of Convergence Science and Technology, Seoul National University**

**August, 2017**

**Approved by thesis committee :**

**Professor**_____**Chairperson**

**Professor**_____**Vice Chairperson**

**Professor**_____

**Professor**_____

**Professor**_____

## ABSTRACT

# Disruption of CTCF/cohesin-mediated high-order chromatin structures by DNA methylation downregulates PTGS2 expression

**Jee-Youn Kang**

**Department of Molecular Medicine**

**and Biopharmaceutical Sciences**

**World Class University Graduate School**

**of Convergence Science and Technology**

**Seoul National University**

The CCCTC-binding factor (CTCF)/cohesin complex regulates gene

transcription via high-order chromatin organization of the genome. *De novo* methylation of CpG islands in the promoter regions is an epigenetic hallmark of gene silencing in cancer. Although the CTCF/cohesin complex preferentially targets hypomethylated DNA, it remains unclear if CTCF/cohesin-mediated high-order chromatin structure is affected by DNA methylation during tumorigenesis. We found that DNA methylation down-regulates expression of prostaglandin-endoperoxidesynthase 2 (*PTGS2*), which is an inducible, rate-limiting enzyme for prostaglandin synthesis, by disrupting CTCF/cohesin-mediated chromatin looping. We show that the CTCF/cohesin complex is enriched near a CpG island associated with *PTGS2*. The *PTGS2* locus forms chromatin loops through methylation-sensitive binding of the CTCF/cohesin complex. However, DNA methylation abolishes the association of the CTCF/cohesin complex with the *PTGS2* CpG island. Disruption of chromatin looping by DNA methylation abrogates the enrichment of transcriptional components, such as positive elongation factor b, at the transcriptional start site of the *PTGS2* locus. These alterations result in the down-regulation of *PTGS2*. Our results provide evidence that CTCF/cohesin-mediated chromatin looping of the *PTGS2* locus is dynamically influenced by the DNA methylation status.

**Keywords:** DNA methylation; PTGS2; CTCF; cohesin; high-order chromatin structures; chromosome conformation capture

**Student number : 2014-30804**

# CONTENTS

**ABSTRACT** ····· i

**CONTENTS** ····· iii

**LIST OF TABLES** ····· iv

**LIST OF FIGURES** ····· v

**INTRODUCTION** ····· 1

**MATERIALS AND METHODS** ····· 4

**RESULTS** ····· 8

**DISCUSSION** ····· 34

**REFERENCES** ····· 37

**ABSTRACT IN KOREAN** ····· 44

# LIST OF TABLES

**Table 1. Primer sequences for quantitative real time PCR··6**

**Table 1. Primer sequences for ChIP-PCR·····8**

# LIST OF FIGURES

**Figure 1. The spatial chromatin organization of the *PTGS2* locus by methylation-sensitive binding of CTCF/cohesin.‥14**

**Figure 2. De-methylation of the *PTGS2* CpG island restores the spatial organization of the *PTGS2* locus.……19**

**Figure 3. Cohesin depletion reduces *PTGS2* expression by abolishing proper spatial chromatin organization of the *PTGS2* locus.……25**

**Figure 4. 5-aza-CdR mediated *PTGS2* mRNA induction was reduced by knockdown of cohesin expression in SNU601 cells.……32**

**Figure 5. Cohesin is required for the formation of organized chromatin at the *PTGS2* locus.……36**

# INTRODUCTION

Genomes are dynamically packaged into a compact three-dimensional nuclear space to form high-order chromatin structures. This packaging occurs in a highly specific manner to facilitate nuclear functions, such as DNA replication, DNA repair, and transcription.[7, 25, 29, 36] Many high-order chromatin structures are established by a special class of architectural proteins, of which CCCTC-binding factor (CTCF) and cohesin are the best characterized.[27] CTCF forms long-range chromatin interactions between enhancers and promoters.[21] Half of the cohesin molecule colocalizes to the same regions with the CTCF-binding sites in the mammalian genome and prior studies have shown that CTCF is required for the recruitment of cohesin to these binding sites.[9, 28, 34] Apart from its major function in sister chromatid cohesion,[10] cohesin affects gene transcription by facilitating long-range chromatin interactions along with CTCF between the members of many developmentally regulated gene families.[35, 37, 46]

Epigenetic modification is a heritable change in gene expression without alterations in DNA sequence and is a hallmark of cancer.[2, 27] DNA methylation of CpG islands in promoter regions is a predominant epigenetic mechanism by which various genes are inactivated during tumorigenesis.[17] CTCF is associated with the transcriptional regulation of several imprinted genes, such as the *IGF2/H19* locus, by preferentially targeting hypomethylated DNA.[3, 18, 33] Thus, aberrant *de novo* DNA methylation may prevent the binding of CTCF to the promoter region, facilitating

transcriptional silencing of the gene. Although genes that may be influenced by this type of regulation have been proposed,[1, 4, 19, 26] there is no direct evidence that CTCF/cohesin-mediated long-range chromatin interactions are disrupted by DNA methylation during tumorigenesis.

Prostaglandin-endoperoxidesynthase 2 (PTGS2, also known as cyclooxygenase-2 or prostaglandin G/H synthase 2) is the inducible form of the rate-limiting enzyme for prostaglandin production.[36] An aberrantly high level of *PTGS2* expression is frequently detected in numerous cancers and other diseases.[36] Conversely, we and others have reported that hypermethylation of the *PTGS2* CpG island directly down-regulates *PTGS2* expression in many human cancers, including gastric and colorectal cancers.[30, 35] Considering that gastric cancers with *PTGS2* CpG island methylation show significantly lower recurrence and improved overall survival,[6] it is important to understand the underlying mechanisms leading to transcriptional silencing of *PTGS2* by DNA methylation.

In the present investigation, we examined if DNA methylation can down-regulate *PTGS2* expression by disrupting CTCF/cohesin-mediated chromatin looping of the *PTGS2* locus. Our data show that enrichment of the CTCF/cohesin complex near the *PTGS2* CpG island is prohibited by DNA methylation. Reduced CTCF/cohesin binding abolishes the spatial proximity between CTCF/cohesin binding sites. As a result, the recruitment of key transcriptional components, such as positive elongation factor b (P-TEFb), are diminished, leading to decreased transcriptional elongation and a low level of *PTGS2* expression. Our findings strongly suggest that DNA methylation down-regulates *PTGS2* expression by disrupting

CTCF/cohesin-mediated high-order chromatin structures.

# MATERIALS AND METHODS

## Cell culture

Cells were obtained from American Tissue Culture Collection or the Korean Cell Line Bank and were not cultured for longer than six months. Cells were cultured in DMEM or RPMI 1640 supplemented with 10% fetal bovine serum and gentamicin (10μg/mL) at 37 °C in a 5% $CO^2$-humidified atmosphere.

## Virus production, and transduction

Control *GFP* and *RAD21*-directed TRC lentiviral shRNAs (#35 and #98) were purchased from Open Biosystems. Lentiviruses were produced by transducing 293FT cells with shRNA using a Virapower packaging mix (Invitrogen) as previously described.[31] Briefly, the viruses were harvested from media on day 3 by centrifugation, and cells were incubated with viral supernatant in the presence of 6 μg/mL polybrene (Sigma). After two days of incubation, transduced cells were cultured in the presence of 1 μg/mL puromycin(Sigma) for another three days before collection as previously described.[16] Silencing was confirmed by western blot analysis and qPCR. Flow cytometry was performed as previously described.[16]

## Bisulfite Sequencing and Pyrosequencing

Genomic DNA (gDNA) samples were isolated using a QIAamp DNA mini kit (Qiagen). gDNA (1 μg) was treated with sodium bisulfite and EpiTech Bisulfite (Qiagen). For bisulfite sequencing, PCR was performed as follows: 95 °C for 10 min, 32 cycles of 95 °C for 20s, 56 °C for 20s, 72 °C for 20s, followed by a final extension at 72 °C for 10 min. The PCR products were gel purified and cloned into a TOPO TA cloning vector (Invitrogen). The inserted PCR fragments of individual clones were sequenced. For pyrosequencing analysis, bisulfite-modified gDNA was amplified with specific primers that were biotinylated. Preparation of single-stranded DNA template, annealing to the pyrosequencing primer, and pyrosequencing were performed using Pyro Gold Q96 SQA reagents with a PyroMark ID pyrosequencer (Qiagen) according to the manufacturer's protocol. The pyrosequencing data were analyzed using Pyro Q-CpG software (Qiagen). All primer sequences for PCR and pyrosequencing are available upon request.

## Reverse transcription and quantitative real-time PCR (qRT-PCR)

Total RNA was prepared using the TRI Reagent (Molecular Research Center) in accordance with the manufacturer's instructions. Briefly, total RNA (2 μg) was reverse transcribed using ImProm-II reverse transcriptase (Promega) and random hexamers as previously described.[30, 31] For quantitative real-time PCR (qRT-PCR), cDNAs were amplified with SYBR Green (Molecular Probes) using StepOnePlus (Applied Biosystems) as previously described.[16]

**Table 1. Primer sequences for quantitative real time PCR**

| GENE | SEQUENCE (5' -> 3') | |
|---|---|---|
| PTGS2 | F | TGAGCATCTACGGTTTGCTG |
| | R | TGCTTGTCTGGAACAACTGC |
| Rad21 | F | TGACTTTGATCAGCCACTGC |
| | R | TCTCACGATCATCCATTCCA |
| CTCF | F | TTACACGTGTCCACGGCGTTC |
| | R | GCTTGTATGTGTCCCTGCTGGCA |

## Chromatin immunoprecipitation (ChIP) assay

ChIP assays were performed as previously described.[31, 46] Briefly, cells were cross-linked with 1% formaldehyde for 10min at room temperature. 0.125M glycine was added for 5min at room temperature to terminate the reaction. Nuclei were prepared and digested with 50 U MNase at 37°C for 15 min, and then were sonicated to yield chromatin fragments of 200–400 bp. The precleared chromatin was overnight incubated with antibodies at 4°C. The chromatin was incubated with protein A agarose (Millipore), which was pre-equilibrated with sonicated salmon sperm DNA and BSA. Immunoprecipitated material was then washed extensively, and the crosslinks were reversed. DNA from eluted chromatin was purified by phenol extraction and ethanol precipitation. qPCR using SYBR Green (Molecular Probes) was performed to observe enriched DNA The enrichment of target DNA over the input was calculated using the ΔΔCt method ,and the results were presented as the mean ± SEM.[16, 31]

**Table 1. Primer sequences for quantitative real time PCR**

| GENE | SEQUENCE (5' -> 3') | |
|---|---|---|
| PTGS2_1 | F | ATGAAACAACCAGCCAAACC |
| | R | CTCCCCCTAGAGGTTGGAGT |
| PTGS2_2 | F | TGCTGGTCATGGGAGTGTAT |
| | R | TTTCCCAACAAATTTCAGACG |
| PTGS2_3 | F | TGTTCTCCGTACCTTCACCC |
| | R | CCGCTTCCTTTGTCCATCAG |
| PTGS2_4 | F | TAGGCTTTGCTGTCTGAGGG |
| | R | ATTTCGTCACATGGGCTTGG |
| PTGS2_5 | F | GTTCCCACCCATGTCAAAAC |
| | R | AAAATTCCGCTGCAAGAAGA |
| PTGS2_6 | F | TGAGCATCTACGGTTTGCTG |
| | R | TGCTTGTCTGGAACAACTGC |
| PTGS2_7 | F | GATTTGAGAGCCCACACCAT |
| | R | CATGCAAACCACACAGAACC |
| Necdin | F | CTGGAGGCAGATGAATGGTT |
| | R | GGTAGCACAAAAGCGAAAGC |
| P21(+1775) | F | AGCCGGAGTGGAAGCAGA |
| | R | AGTGATGAGTCAGTTTCCTGCAAG |

## Chromosome conformation capture (3C) assay

A 3C assay was performed as previously described[7, 34] with minor modification. Briefly, chromatin cross-linked in 1% formaldehyde was digested with 500 U EcoRI (NEB) overnight followed by ligation with 2,000 U of T4 DNA ligase (NEB) at 16°C for 4 h. Cross-linking was reversed, and DNA was purified by phenol extraction and ethanol precipitation as previously described.[31] To generate control templates as positive controls, the BAC clone CTD-3241P15, which covered the entire *PTGS2* locus, was digested with 200 U EcoRI overnight at 37°C as previously described.[32] After phenol extraction and ethanol precipitation, DNA fragments (200 ng/μL) were ligated with T4 DNA ligase. Digestion efficiency was calculated as previously described,[14] and samples with efficiencies >90% were used for 3C assays. Cross-linking frequency and ligation efficiencies between different samples were normalized relative to the ligation frequency of two adjacent digested fragments in the *CalR* gene.[34] Quantification of the data was performed by qPCR using SYBR Green (Molecular Probe). EcoRI restriction sites in the *PTGS2* locus appear as gray, shaded bars. Black shading indicates the anchor fragment of the transcriptional start site of *PTGS2*. The maximum cross-linking frequency was set to 1.

## Antibodies

Antibodies specific for the following were used in this study: PTGS2 (SC-1745), normal rabbit IgG (SC-2027), CDK9 (SC-484), and RNA pol II (SC-899) was purchased from Santa Cruz Biotechnology; Ser2P Pol II (ab5059), H3K4me1 (ab8895), and RAD21 (ab992) were from AbCam, and AcH3 (06-599), CTCF (07-729), H3K4me3 (07-473), and H3K27me2 (07-452) were from Millipore. Anti-SMC1 antibody (A300-055A) was purchased from Bethyl Laboratories.

# RESULTS

## 1. The *PTGS2* locus forms spatial chromatin organization in a methylation-sensitive manner

A bioinformatics search of the UCSC Genome database (http://genome.ucsc.edu/) for CTCF/cohesin binding motifs across the *PTGS2* locus revealed four putative candidate sites (Figure 1a). One of the CTCF/cohesin-binding motifs was located at the transcriptional start site in the *PTGS2* CpG island (amplicons 3 and 4); thus, we speculated that the binding of CTCF/cohesin to the *PTGS2* locus may be influenced by DNA methylation.

To test this hypothesis, we performed chromatin immunoprecipitation (ChIP) assays using two gastric cancer cells with different DNA methylation patterns at the *PTGS2* CpG island. We previously showed that SNU668 cells express a high level of *PTGS2* and are devoid of DNA methylation at the *PTGS2* CpG island. In contrast, SNU601 cells have undetectable *PTGS2* expression and are hypermethylated at the same region (Figures 1b-d).[30] High-resolution ChIP assays showed that CTCF binding occurred at four potential CTCF/cohesin binding sites in the *PTGS2* locus in SNU668 cells with an unmethylated *PTGS2* CpG island (black bars; amplicons 1, 2, 4, and 7) (Figure 1e). Prominent binding of RAD21, a core subunit of the cohesin complex,[8] colocalized with CTCF at the *PTGS2* locus in SNU668

cells (Figure 1f). However, despite similar binding patterns at most putative CTCF/cohesin-binding sites in the *PTGS2* locus, recruitment of CTCF and RAD21 near the transcriptional start site of the *PTGS2* locus in SNU601 cells (red bars; amplicons 3, 4, and 5) was significantly less than that of SNU668 cells (Figures 1e and f). This difference in recruitment suggests that hypermethylation of the *PTGS2* CpG island disrupted the binding of methylation-sensitive CTCF/cohesin at these sites in SNU601 cells. Consistent with active transcription of *PTGS2* in SNU668 cells (Figures 1b and c), the binding of CTCF and cohesin at the transcriptional start site in the *PTGS2* CpG island coincided with the enrichment of the active histone marker, H3K4 tri-methylation (H3K4me3)[27] (Figure 1g). Repressive histone H3K27 di-methylation (H3K27me2)[27] was enriched in SNU601 cells with a methylated *PTGS2* CpG island (Figure 1h). Similarly, CTCF/cohesin-binding sites were strongly enriched for histone H3K4 mono-methylation (H3K4me1), which is apredictive marker of enhancers,[15] in SNU668 cells (Figure 1i). These data demonstrate that the CTCF/cohesin complex is localized at the CTCF/cohesin-binding sites of the *PTGS2* locus in SNU668 cells express a high level of *PTGS2*. However, hypermethylation of the *PTGS2* CpG island disrupts the binding of the methylation-sensitive CTCF/cohesin complex on these sites in SNU601 cells with methylated *PTGS2*.

Recent evidence indicates that CTCF and cohesin mediate long-range chromatin interactions at CTCF/cohesin-binding sites at the *IFNG*, *IGF2-H19*, and *β-globin* loci.[13, 16, 21] To test whether the *PTGS2* locus can form long-range chromatin interactions through CTCF/cohesin-binding, we performed chromosome conformation capture (3C) assays[7] with the EcoRI

restriction enzyme to assess chromatin interactions across the *PTGS2* locus (Figure 1j). The transcriptional start site of the *PTGS2* locus strongly interacted with the CTCF/cohesin-binding sites at −42.5 kb and +74.5 kb in SNU668 cells, which display a high level of *PTGS2* expression (black line, Figure 1j); no interactions were detected at other sites without CTCF/cohesin enrichment. The physical proximity of CTCF/cohesin-binding sites in SNU601 cells (red line, Figure 1j) was significantly lower than that of SNU668 cells. Thus, CTCF/cohesin may form long-range chromatin interactions at the *PTGS2* locus to facilitate transcription and a high level of *PTGS2* expression in SNU668 cells. In contrast, DNA methylation of the *PTGS2* CpG island in SNU601 cells may abolish CTCF/cohesin-mediated spatial organization, resulting in transcriptional inefficiency.

We also compared the methylation status, CTCF/cohesin binding, and spatial chromatin organization of the *PTGS2* locus in A549 and SNU719 cells. The A549 cells exhibits a methylation pattern similar to that of SNU668 cell, whereas, SNU719 cells demonstrate a methylation pattern similar to that of SNU601 cells. As expected, our results in A549 and SNU719 cells were similar to the previous results obtained from SNU668 and SNU601 cells. These data suggest that the inhibitory effect of DNA methylation on CTCF/cohesin-mediated high-order chromatin structures at the *PTGS2* locus may be generalized to other cell lines.

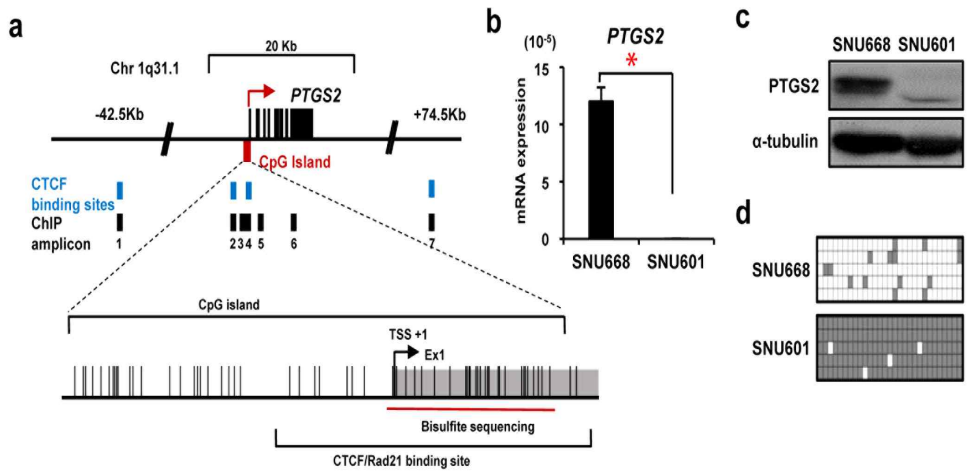


**Figure 1. The spatial chromatin organization of the *PTGS2* locus by methylation-sensitive binding of CTCF/cohesin.** (a) The *PTGS2* locus at chromosome 1q31.1 is illustrated to scale. The location of putative CTCF/cohesin-binding sites and the primer pairs used for quantitative real-time PCR (qPCR) are shown with labels below. The *PTGS2* CpG island is also shown. Exon1 is indicated by a gray box. Vertical bars represent each CpG site. TSS, transcriptional start site. (b) *PTGS2* mRNA expression in SNU668 and SNU601 cells was analyzed by qRT-PCR and normalized relative to 18S ribosomal RNA. Data are presented as the mean ± SD of triplicate independent RNA preparations. *P<0.05, **P<0.001. (c) Western blot analysis was performed with anti-PTGS2 antibody; a-tubulin served as a loading control. (d) Bisulfite sequencing analysis of the *PTGS2* CpG island in SNU668 and SNU601 cells is shown. Each square denotes a CpG site within the PCR product amplified from bisulfite-treated DNA.[38] (Filled squares: methylated; open squares: unmethylated).

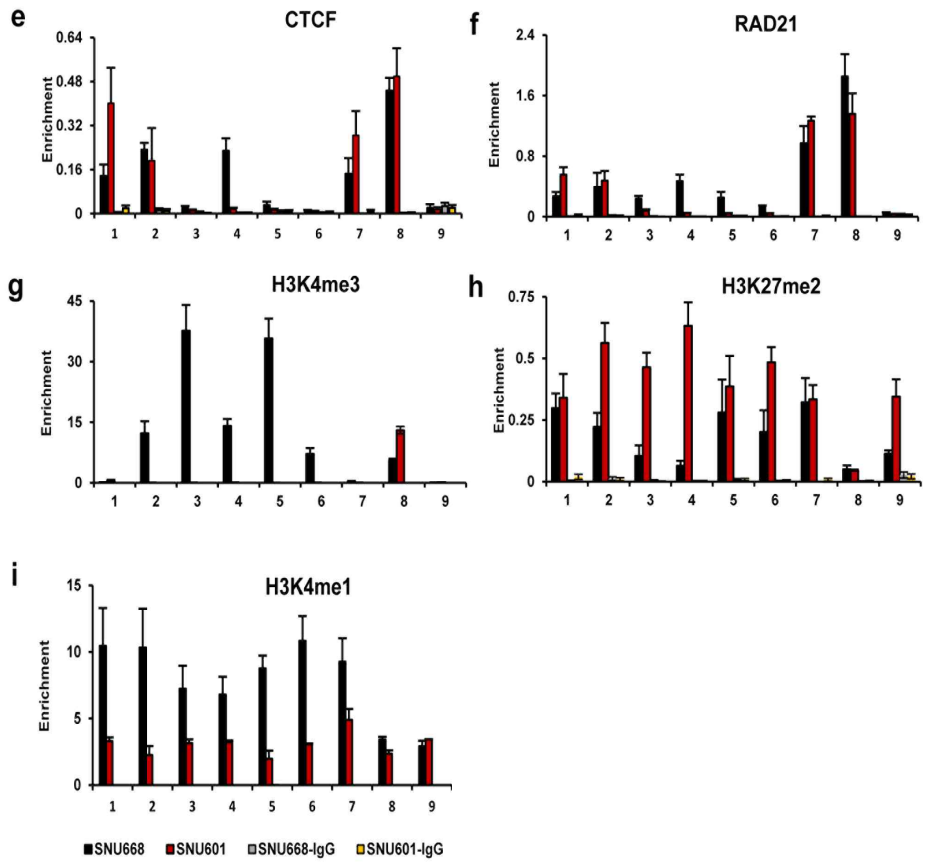


**Figure 1.** (e-i) A ChIP assay was performed with SNU668 (black bars) or SNU601 (red bars) cells using antibodies against (e) CTCF, (f) RAD21, (g) H3K4me3, (h) H3K27me2, and (i) H3K4me1. qRT-PCR using SYBR Green was performed to detect enriched DNA. Enrichment of target DNA over input was calculated using the ΔΔCt method,[16, 31] and results are represented as the mean ± SEM, n = 3. The +1775 site (amplicon 8) of the *P21* locus[12] and *NECDIN* (amplicon 9)[31] served as positive and negative controls, respectively, for CTCF/cohesin binding.

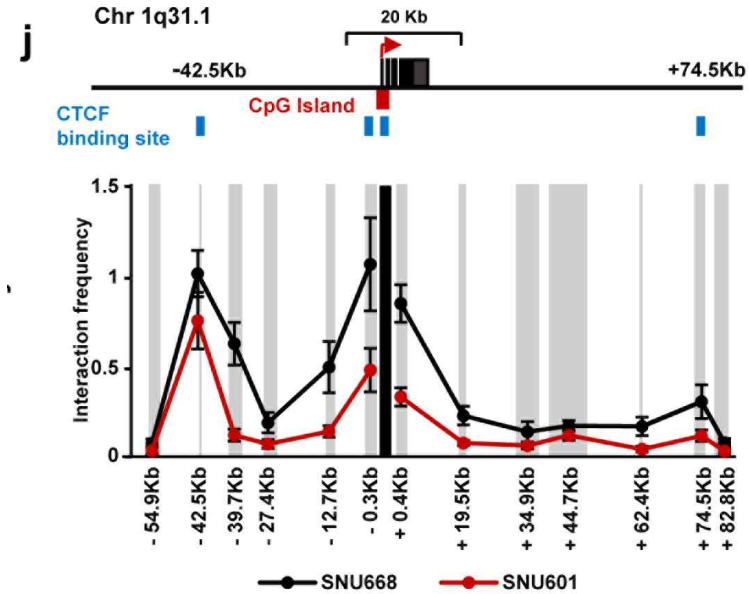


**Figure 1.** (j) Relative cross-linking frequencies among CTCF/cohesin-binding sites in the *PTGS2* locus were measured with a 3C assay[7] in SNU668 (black line) and SNU601 (red line) cells. Chromatin cross-linked in 1% formaldehyde was digested with the restriction enzyme EcoRI overnight, followed by ligation with T4 DNA ligase at 16°C for 4h.[16, 31, 34] Cross-linking was reversed, and the DNA was purified as previously described.[31] Cross-linking frequencies and ligation efficiencies between different samples were normalized relative to the ligation frequency of two adjacent digested fragments in the *CalR* gene.[34] Quantification of data was performed by qPCR using SYBR Green. EcoRI restriction sites in the *PTGS2* locus appear as gray, shaded bars. Black shading indicates the anchor fragment of the transcriptional start site of *PTGS2*. The maximum cross-linking frequency was set to 1 (mean ± SEM, n = 4).

## 2. DNA methylation reduces the spatial organization of the *PTGS2* locus

We examined whether DNA methylation abrogates transcription by disrupting the binding of CTCF/cohesin to the *PTGS2* locus. We determined the dynamics of CTCF and cohesin binding after treatment of SNU601 cells with the demethylating agent, 5-Aza-2'-deoxycytidine (5-aza-CdR).[38]

Treatment with 5-aza-CdR caused a dose-dependent reactivation of *PTGS2* mRNA expression in SNU601 cells (Figure 2a). Pyrosequencing analysis of SNU601 cells treated with 500 nM 5-aza-CdR demonstrated reduced DNA methylation at the *PTGS2* CpG island (Figure 2b), confirming the importance of DNA methylation in the transcriptional repression of *PTGS2*.[30] Next, ChIP assay with antibodies against CTCF and cohesin was performed on SNU601 cells treated with 500 nM 5-aza-CdR (Figures 2c and d). Demethylation of the *PTGS2* CpG island by 5-aza-CdR treatment (Figures 2a and b) resulted in increased binding of CTCF and cohesin at the *PTGS2* CpG island (red bars; amplicons 3, 4, and 5 in Figures 2c and d). Binding of CTCF and cohesin at this region was undetectable in DMSO-treated SNU601 cells (black bars; Figures 2c and d); thus, we concluded that CTCF and cohesin binding was influenced by the methylation status of the *PTGS2* CpG island.

Because G9A- and EZH2-mediated histone modification cooperates with DNA methyltransferases to silence *PTGS2* expression,[5] we asked if 5-aza-CdR treatment changed the epigenetic signatures within the *PTGS2* locus. Upon 5-aza-CdR treatment, the binding of active H3K4me3 within the *PTGS2* locus was enhanced by approximately 10-fold (Figure 2e) in parallel

with increased transcription of *PTGS2* (Figure 2a). Interestingly, the repressive H3K27me2 mark throughout the *PTGS2* locus was also slightly enriched after 5-aza-CdR treatment (Figure 2f), consistent with the previous observation that promoter regions of demethylated genes are frequently marked by bivalent histone modifications in human cancer cells.[9, 20] Taken together, the binding of CTCF and cohesin to their binding sites at the transcriptional start site of *PTGS2* was regulated by DNA methylation within the *PTGS2* CpG island.

Consistent with the increased enrichment of CTCF and cohesin (Figures 2c and d), the physical proximity of the *PTGS2* locus in the 5-aza-CdR treated SNU601 cells (red line, Figure 2g) was significantly increased compared to that in control DMSO-treated cells (black line, Figure 2g). These results suggest that DNA methylation of the *PTGS2* CpG island in SNU601 cells abolishes CTCF/cohesin-mediated spatial organization of the *PTGS2* locus..

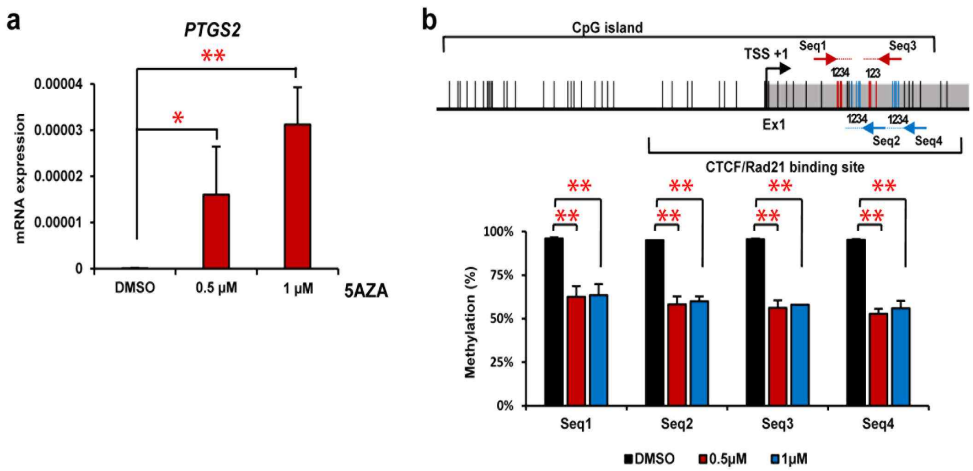


**Figure 2. De-methylation of the *PTGS2* CpG island restores the spatial organizatin of the *PTGS2* locus.** (a) SNU601 cells were treated with 500 nM or 1mM 5-aza-CdR for 4 days, and *PTGS2* mRNA levels were analyzed with qRT-PCR and normalized to 18S ribosomal RNA (mean ± SD, n = 4). *P<0.05,**P<0.001. (b) SNU601 cells were treated with 500 nM or 1mM 5-aza-CdR for 4 days, followed by genomic DNA preparation. For pyrosequencing analysis,[38] bisulfite-modified genomic DNA was amplified with specific biotinylated primers. Quantitative analysis of the *PTGS2* CpG island methylation was performed using a PyroMark ID pyrosequencer (Qiagen) as previously described.[38] Locations of sequences corresponding to the four primer sets used for pyrosequencing are indicated by arrows. The y-axis represents the percentage of CpG methylation of each sequence (mean ± SD, n= 3). *P<0.05, **P<0.001.

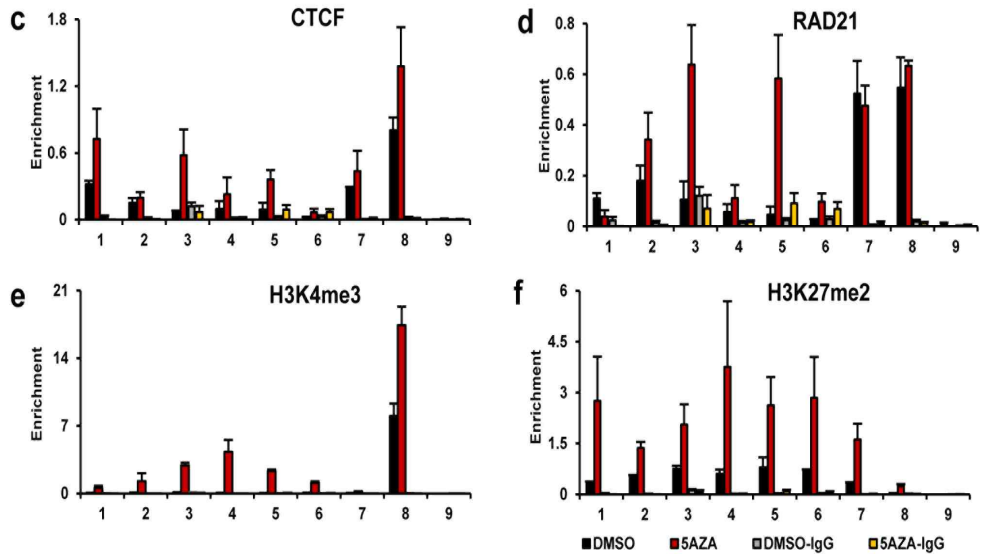


**Figure 2.** (c-f) SNU601 cells were treated with DMSO (black bars) or 500 nM 5-aza-CdR (red bars) for 4 days, and the ChIP assay was performed using antibodies against (c) CTCF, (d) RAD21, (e) H3K4me3, and (f) H3K27me2. qRT-PCR using SYBR Green was performed to detect enriched DNA. Enrichment of target DNA over input was calculated using the ΔΔCt method,[16, 31] and results are represented as the mean ± SEM, n = 4. The +1775 site (amplicon 8) of the *P21* locus[12] and *NECDIN* (amplicon 9)[31] served as positive and negative controls, respectively, for CTCF/cohesin binding.

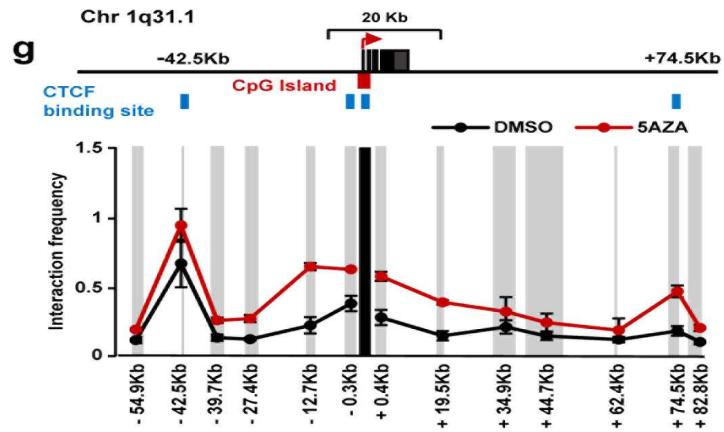


**Figure 2.** (g) Relative cross-linking frequencies among CTCF/cohesin-binding sites in the *PTGS2* locus were measured with a 3C assay[7] in SNU601 cells after treatment with DMSO (black line) or 500 nM 5-aza-CdR (redline) for 4 days. EcoRI restriction sites in the *PTGS2* locus appear as gray, shaded bars. Black shading indicates the anchor fragment of the transcriptional start site of *PTGS2*. The maximum cross-linking frequency was set to 1 (mean ± SEM, n = 5).

## 3. Cohesin binding is crucial for the spatial organization of the *PTGS2* locus

To test if CTCF/cohesin binding is a prerequisite for efficient transcription of *PTGS2*, we reduced the expression of cohesin using *RAD21* knockdown (KD) in SNU668 cells. Two different *RAD21*-specific shRNAs reduced RAD21 expression with a similar efficiency, decreasing *RAD21* mRNA and protein levels by approximately 90% in SNU668 cells (Figures 3a and d). Using fluorescence-activated cell sorting (FACS) analysis we observed that *RAD21*-KD SNU668 cells exited mitosis, divided, and survived well without pronounced levels of cell death (Figure 3e), which is consistent with earlier data.[22, 29] Notably, *PTGS2* mRNA and protein expression were significantly reduced by *RAD21*-KD in SNU668 cells (Figures 3b and c). We obtained similar results after *RAD21*-KD in A549, HeLa, and N87 cancer cells, which have high levels of *PTGS2* expression (Figure 3f). Furthermore, although *PTGS2* expression was induced by phorbol12-myristate 13-acetate (PMA) treatment in control SNU668 cells,[11] we found that PMA-induced *PTGS2* expression was completely abrogated in *RAD21*-KD SNU668 cells (Figure 3g); these data suggest that cohesin is crucial for optimal expression of *PTGS2* in human cancer cells.

Next, we determined if cohesin is essential for long-range chromatin interactions (Figure 1j). Our ChIP experiments showed that *RAD21*-KD resulted in a two-fold reduction in the prominent binding between RAD21 and Structural Maintenance of Chromosomes 1 (SMC1), two members of the

cohesin complex,[8] at the *PTGS2* locus (Figure 3h). These results suggest that *RAD21*-KD blocks the formation and enrichment of the cohesin complex at the *PTGS2* locus in SNU668 cells. However, *RAD21*-KD had no significant effect on the expression or binding of CTCF at the *PTGS2* locus (Figure 3h); this finding supports the paradigm that CTCF binds to chromatin independently of cohesin.[23, 37] Using the 3C assay with *RAD21*-KD SNU668 cells, we found that the spatial proximity in the *RAD21*-KD SNU668 cells (red line, Figure 3i) was significantly lower (two-fold) than that in the control *GFP*-KD SNU668 cells (black line, Figure 3i). We also identified that re-establishment of CTCF/cohesin mediated high-order chromatin structures after the 5-aza-CdR treatment was significantly abolished after Rad21 knockdown (Figure 4). Consequently, re-expression of PTGS2 mRNA after the 5-aza-CdR treatment was also abrogated (Figure 4). These data argue that cohesin binding is required for the long-range chromatin interactions among CTCF/cohesin-binding sites in the *PTGS2* locus.

Next, we examined how cohesin-mediated spatial chromatin organization affects *PTGS2* expression. We examined enrichment of the elongation-competent form of RNA pol II (Pol II), which is phosphorylated at Ser2 of the C-terminal domain (Ser2P), in *RAD21*-KD SNU668 cells.[10] The binding of Ser2P Pol II was significantly decreased throughout the coding region of the *PTGS2* locus in *RAD21*-KD SNU668 cells (Figure 3h), which was consistent with the reduced expression of *PTGS2* (Figure 3b). We found that CDK9, a subunit of the P-TEFb complex that catalyzes phosphorylation of Ser2P,[10] was also reduced at these sites by approximately

two-fold in *RAD21*-KD SNU668 cells (Figure 3h). These data confirm previous observations that cohesin facilitates the transition of paused Pol II to elongation.[29] In addition, the binding of acetylated histone H3 (AcH3), a marker of active transcription,[27] was present within the *PTGS2* locus, although it was reduced by two-fold at these sites in the *RAD21*-KD SNU668 cells (Figure 3h).

Together, these results suggest that cohesin-mediated spatial chromatin organization of the *PTGS2* locus is required for recruitment of the transcription regulator P-TEFb to enhance elongation of *PTGS2* transcripts.

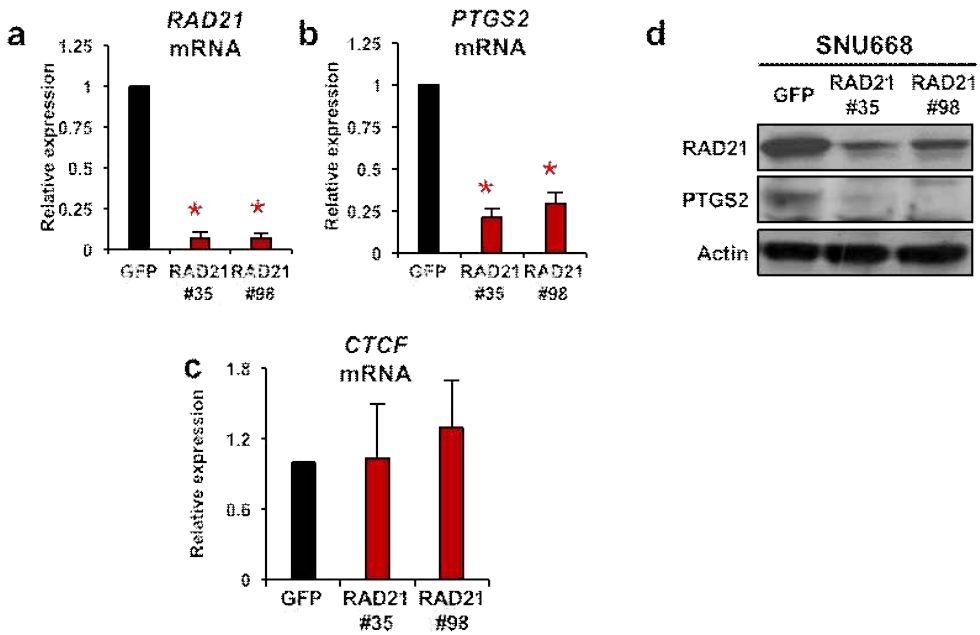


**Figure 3. Cohesin depletion reduces *PTGS2* expression by abolishing proper spatial chromatin organization of the *PTGS2* locus.** SNU668 cells were transduced with control (*GFP*) shRNA or two different *RAD21* shRNAs (#35 and #98) for five days. Lentiviruses were produced as previously described.[31] (a) *RAD21*and (b) *PTGS2* mRNA expression levels were analyzed with qRT-PCR and normalized to that of 18S ribosomal RNA relative to control *GFP-shRNA*-expressing cells. (c) *CTCF* mRNA expression was also analyzed to show *RAD21* knockdown does not affect *CTCF* mRNA expression. Data are the mean ± SD of triplicate independent viral transduction experiments.*P<0.05, **P<0.001. (d) Western blot analysis was performed with anti-RAD21 and anti-PTGS2 antibodies on day 5 after *RAD21*-KD; α-tubulin served as a loading control.

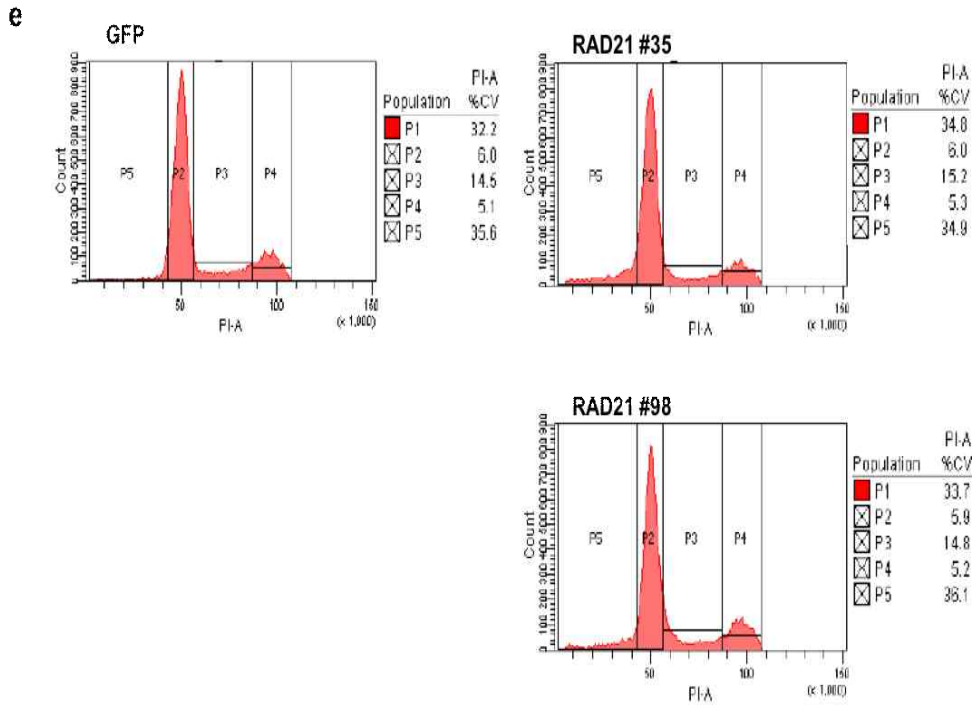


**Figure 3.** (e) Cells were stained with propidium iodide on day 5 after *RAD21*-KD and subjected to FACS analysis. A representative image of the percentage of cells in the G0, G1, S, and G2/M phases is shown.

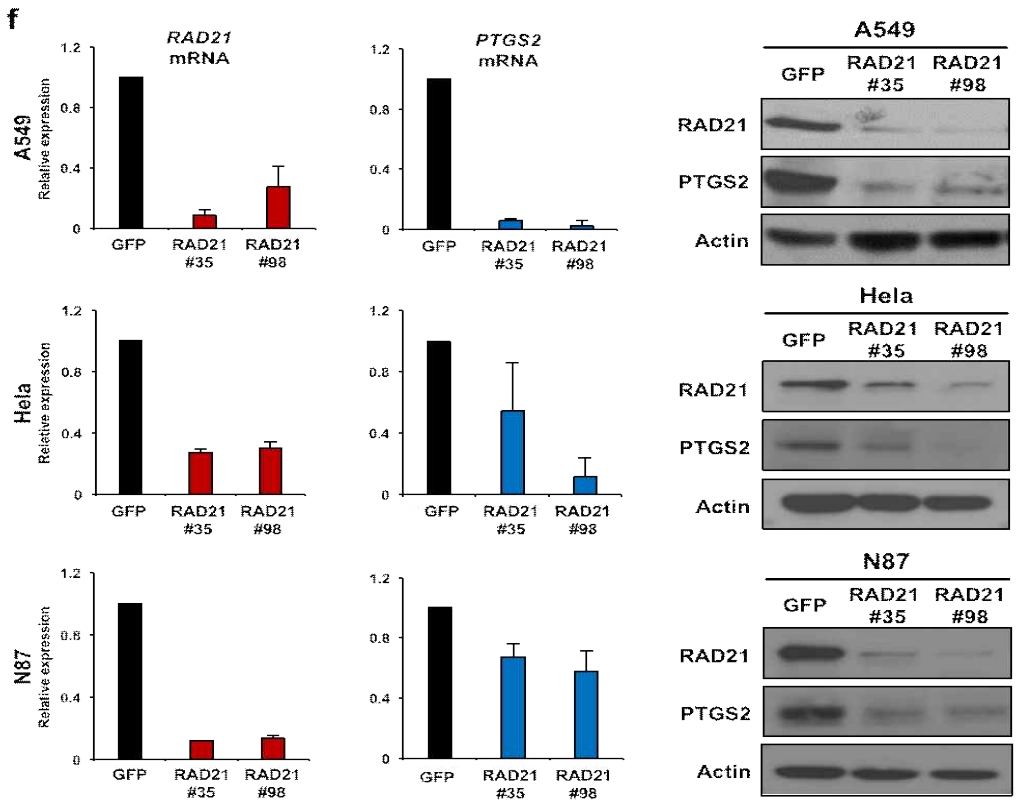


**Figure 3.** (f) Down-regulation of cohesin by *RAD21*-KD reduced *PTGS2* expression in A549, Hela, and N87 cells. A549 (upper panels), HeLa (middle panels), and N87 (lower panels) cells were transduced with *GFP* or two different *RAD21* shRNAs (#35 and #98) for 5 days. *RAD21* and *PTGS2* mRNA expression levels were analyzed with qRT-PCR and normalized to that of 18S ribosomal RNA relative to the *GFP* shRNA-expressing cells. Data are expressed as the mean ± SD of triplicate independent viral transduction experiments. Western blot analysis was performed on A549, HeLa, and N87 cell extracts with RAD21 and PTGS2 antibodies on day 5 after *RAD21*-KD with a-tubulin serving as a loading control.

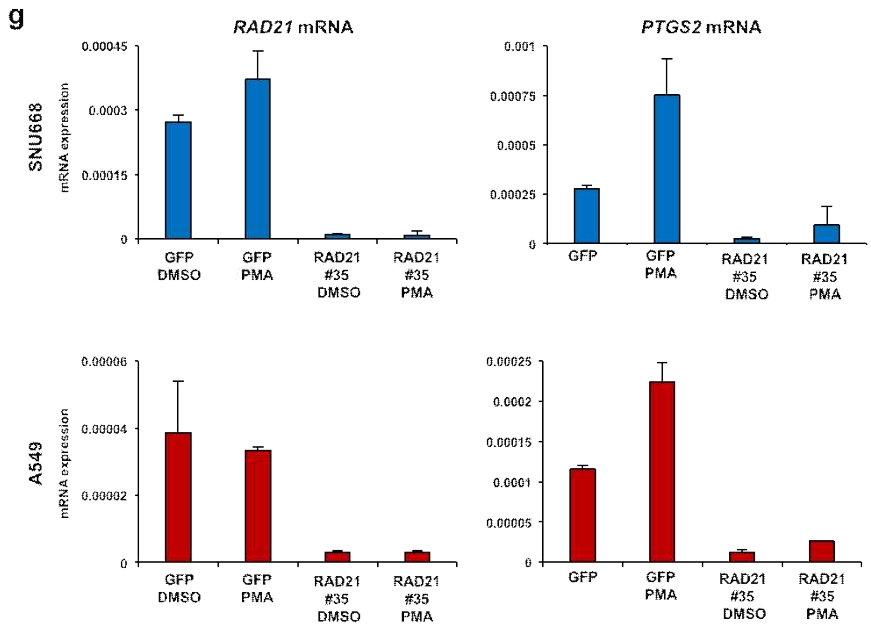


**Figure 3.** (g) PMA-mediated *PTGS2* mRNA induction was inhibited by reduction of cohesin expression in SNU668 and A549 cells. SNU668 and A549 cells were transduced with control *GFP* or *RAD21 shRNA* (#35). On day 5 after *RAD21*-KD, cells were treated with 100ng/ml phorbol 12-myristate 13-acetate (PMA, Sigma) or DMSO for 24 h. *RAD21* and *PTGS2* mRNA expression levels were analyzed with qRT-PCR and normalized to 18S ribosomal RNA. Data are the mean ± SD of triplicate independent viral transduction experiments.

h

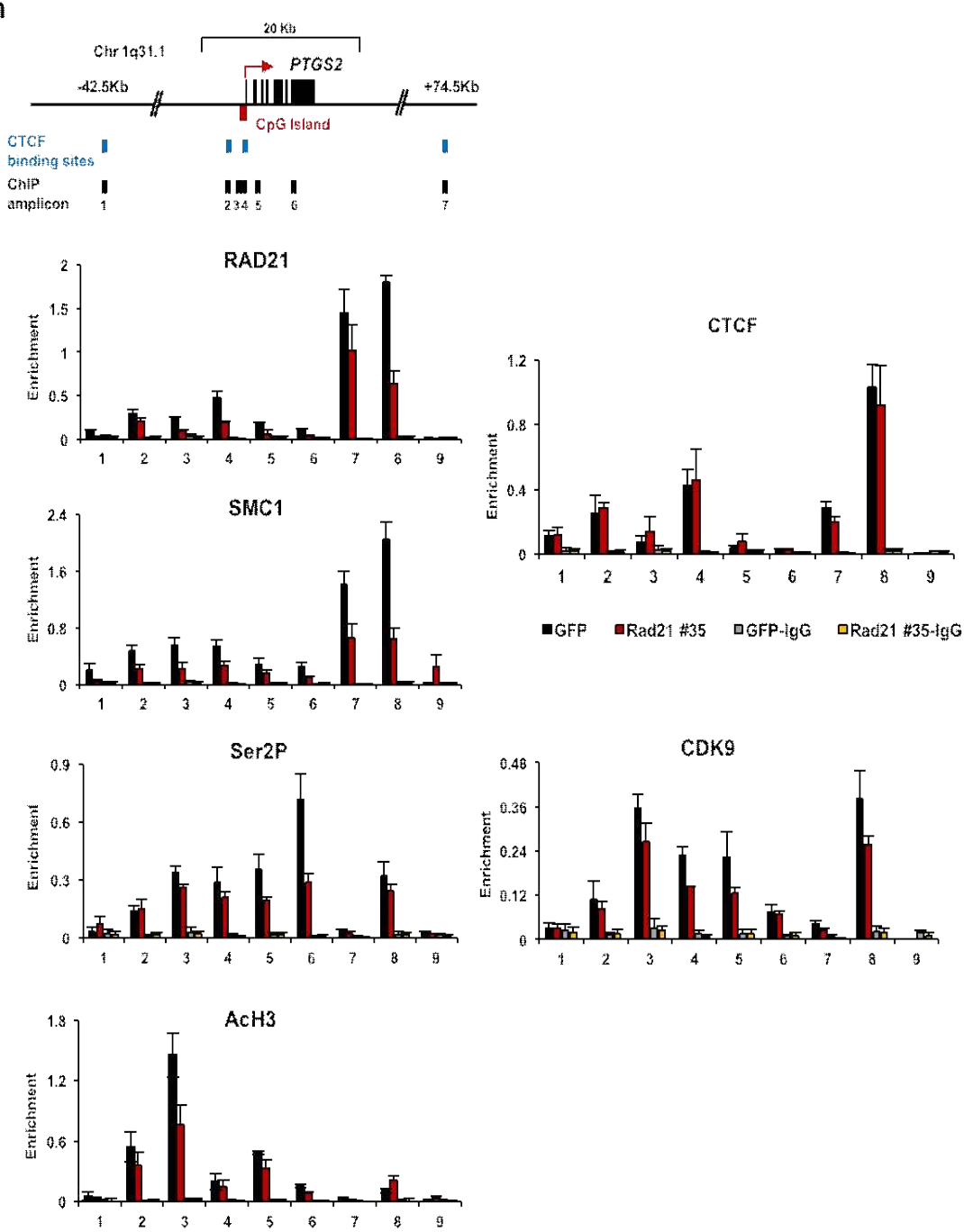
20 Kb
Chr 1q31.1
PTGS2
-42.5Kb
+74.5Kb
CpG Island
CTCF binding sites
ChIP amplicon
1
2 3 4 5
6
7
RAD21
SMC1
CTCF
Ser2P
CDK9
AcH3
Enrichment
GFP
Rad21 #35
GFP-IgG
Rad21 #35-IgG

**Figure 3.** (h) A ChIP assay was performed with *GFP*-KD (black bars) or *RAD21*-KD SNU668 (#35; red bars) cells on day 5 after *RAD21*-KD using antibodies against RAD21, SMC1, CTCF, Ser2P, CDK9, and AcH3 (mean ± SEM, n = 3).

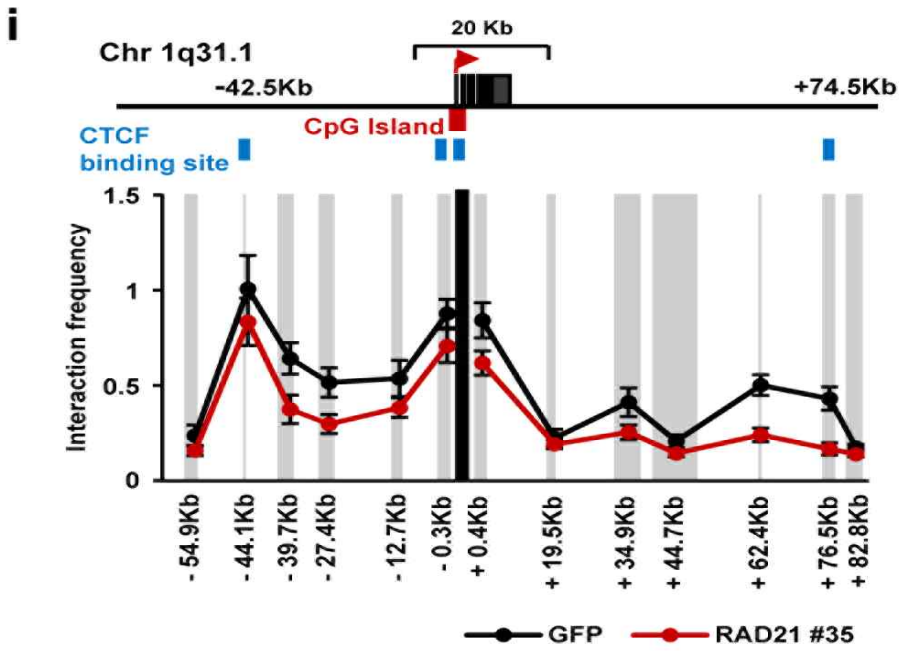


**Figure 3.** (i) Long-range interactions at the *PTGS2* locus were assessed with a 3C assay using *GFP*-KD (black line) or *RAD21*-KD SNU668 (red line) cells. EcoRI restriction sites in the *PTGS2* locus appear as gray, shaded bars. Black shading indicates the anchor fragment of the transcriptional start site of *PTGS2*. The maximum cross-linking frequency was set to 1 (mean ± SEM, n = 5).

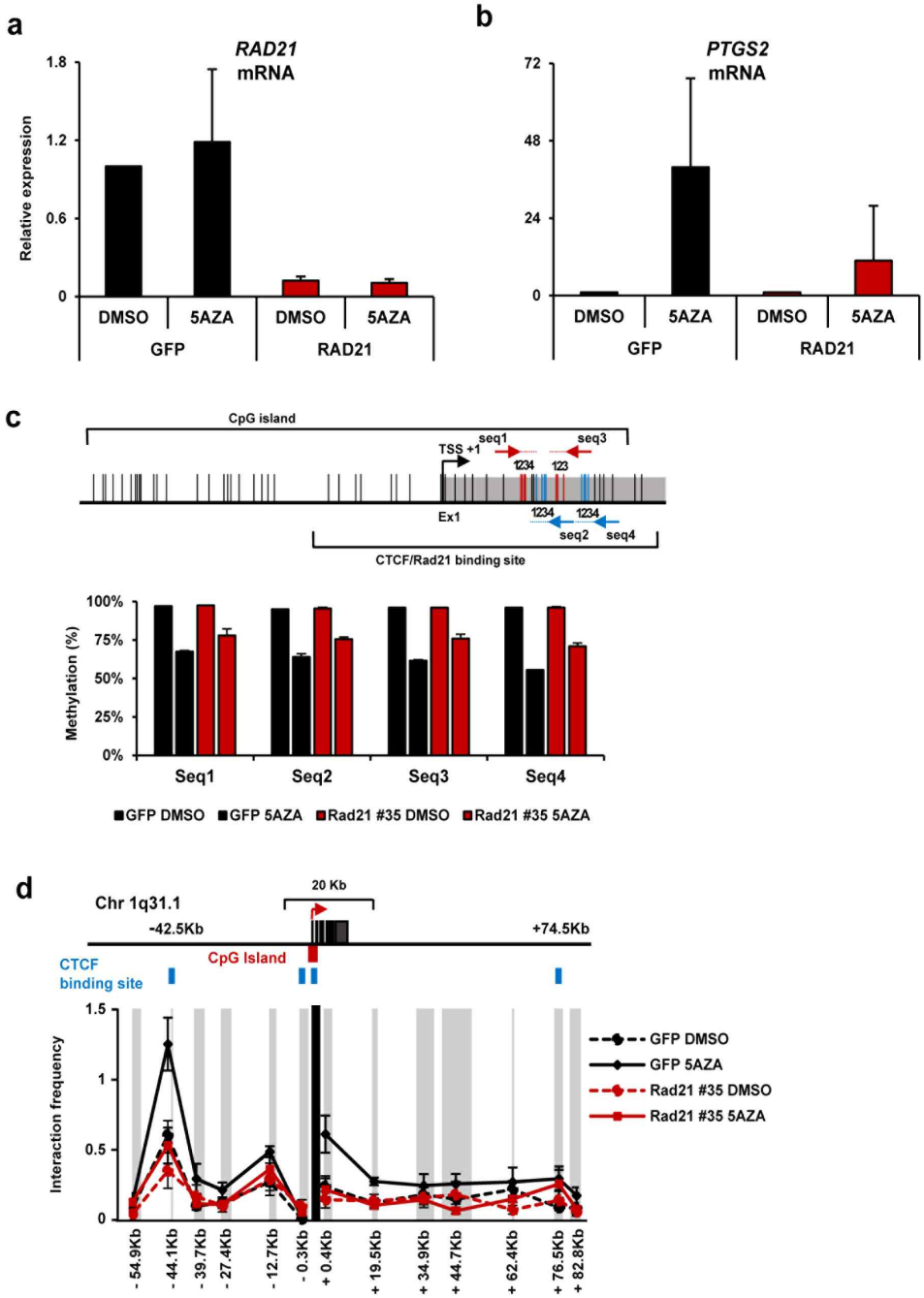
a
RAD21
mRNA
Relative expression
1.8
1.2
0.6
0
DMSO
5AZA
DMSO
5AZA
GFP
RAD21
b
PTGS2
mRNA
72
48
24
0
DMSO
5AZA
DMSO
5AZA
GFP
RAD21
c
CpG island
TSS +1
seq1
seq3
1234
123
Ex1
1234
1234
seq2
seq4
CTCF/Rad21 binding site
Methylation (%)
100%
75%
50%
25%
0%
Seq1
Seq2
Seq3
Seq4
GFP DMSO
GFP 5AZA
Rad21 #35 DMSO
Rad21 #35 5AZA
d
Chr 1q31.1
20 Kb
-42.5Kb
+74.5Kb
CTCF
binding site
CpG Island
Interaction frequency
1.5
1
0.5
0
- 54.9Kb
- 44.1Kb
- 39.7Kb
- 27.4Kb
- 12.7Kb
- 0.3Kb
+ 0.4Kb
+ 19.5Kb
+ 34.9Kb
+ 44.7Kb
+ 62.4Kb
+ 76.5Kb
+ 82.8Kb
GFP DMSO
GFP 5AZA
Rad21 #35 DMSO
Rad21 #35 5AZA

**Figure 4. 5-aza-CdR mediated *PTGS2* mRNA induction was reduced by knockdown of cohesin expression in SNU601 cells.** SNU601 cells were transduced with control *GFP* or *RAD21 shRNA* (#35). On day 5 after *RAD21*-KD, cells were treated with DMSO or 500nM 5-aza-CdR for 4 days. (a) *RAD21* and (b) *PTGS2* mRNA expression levels were analyzed with qRT-PCR and normalized to 18S ribosomal RNA relative to the *GFP*-shRNA expressing cells. Data are the mean ± SD of triplicate independent viral transduction experiments. (c) Bisulfite-treated gDNA was used to determine the methylation ratio of the *PTGS2* CpG island by pyrosequencing (mean ± SD, n = 3). (d) Long-range interactions at the *PTGS2* locus were assessed with a 3C assay using *GFP* or *RAD21*-KD (R#35) SNU601 cells after treatment with DMSO or 500nM 5-aza-CdR for 4 days (mean ± SEM, n = 3).

# DISCUSSION

## Cohesin-mediated chromatin looping is essential for *PTGS2* expression

In the present investigation, we found that CTCF/cohesin-mediated spatial chromatin organization is an essential mechanism for transcriptional regulation of *PTGS2* (Figure 5). Deregulation of CTCF/cohesin binding by DNA methylation may disrupt the proper spatial chromatin organization of the *PTGS2* locus, which subsequently reduces overall *PTGS2* expression. We found that down-regulation of cohesin abolished the proximity among the CTCF/cohesin-binding sites without disturbing CTCF enrichment in *RAD21*-KD cells (Figure 3i). CTCF positions cohesin at the cohesin-binding sites.[23, 28] CTCF binds to the *PTGS2* CpG island in a DNA methylation-sensitive manner (Figure 1e). Thus, we propose that DNA methylation abrogates spatial chromatin organization of the *PTGS2* locus by disrupting both CTCF and cohesin binding, both of which are indispensable for direct interactions among CTCF/cohesin-binding sites. Considering the recent discovery that aberrant overexpression of the cohesin component is frequently detected in many human cancers,[24] this raises the possibility that activated CTCF/cohesin mediates *PTGS2* up-regulation, which is associated with tumor progression. Thus, hypomethylation of *PTGS2* may confer an obvious advantage to cancer cells by increasing and maintaining elevated

levels of *PTGS2* during tumor development.[25]

Our results provide evidence that cohesin-mediated spatial chromatin organization can be abolished by DNA methylation at the *PTGS2* CpG island; this finding highlights a mechanistic linkage between high-order chromatin structures and DNA methylation during tumorigenesis. Our findings correlate with a previous result that gastric cancer patients with methylated *PTGS2* show lower recurrence and improved overall survival rates compared to those of patients with unmethylated *PTGS2*.[6] Thus, future studies should be performed to determine the detailed mechanism by which DNA methylation affects this dynamic transition of the high-order chromatin landscape during tumor progression; such studies will ultimately allow new, effective epigenetic therapies to be developed.

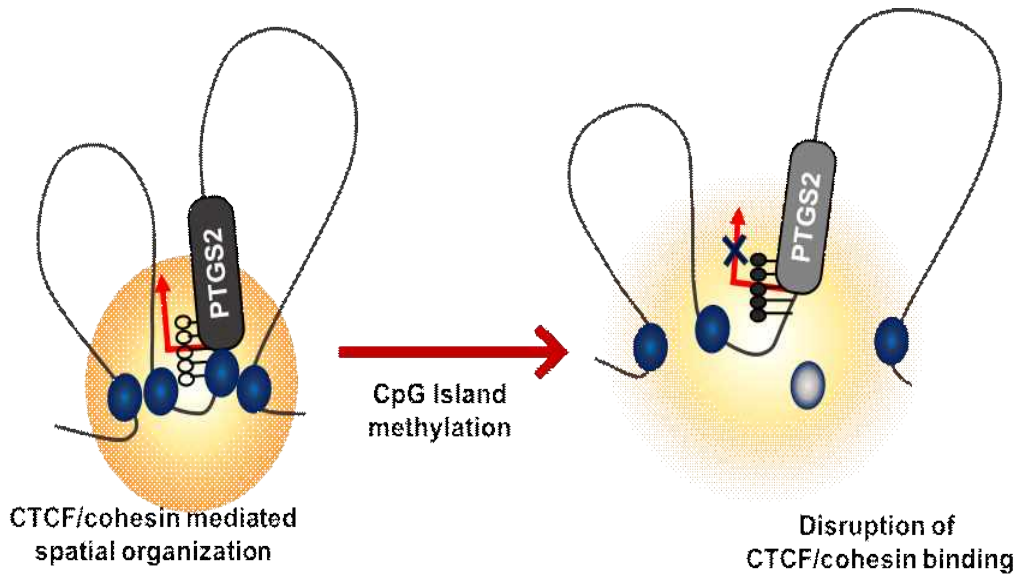


**Figure 5. Cohesin is required for the formation of organized chromatin at the *PTGS2* locus.** A proposed model for stabilizing high-level *PTGS2* expression by cohesin-mediated chromatin looping is shown. The *PTGS2* locus forms chromatin loops in cancer cells that express high levels of *PTGS2* (left). CTCF/cohesin (blue ovals) stabilizes long-range chromatin interactions through direct interactions at CTCF/cohesin localization sites. DNA methylation of the *PTGS2* CpG island abolishes the association among CTCF/cohesin-binding sites at the *PTGS2* locus by inhibiting the enrichment of CTCF/cohesin at these regions (right, grey oval). Deregulation of chromatin organization at the *PTGS2* locus decreases the association of the transcription regulator P-TEFb near these regions, reducing *PTGS2* expression in cancer cells with heavily methylated CpG islands.

# REFERENCES


1 Batlle-Lopez A, Cortiguera MG, Rosa-Garrido M, Blanco R, Del Cerro E, Torrano V *et al*. Novel CTCF binding at a site in exon1A of BCL6 is associated with active histone marks and a transcriptionally active locus. Oncogene 2013.

2 Baylin SB, Jones PA. A decade of exploring the cancer epigenome – biological and translational implications. Nature reviews Cancer 2011; 11: 726-734.

3 Bell AC, Felsenfeld G. Methylation of a CTCF-dependent boundary controls imprinted expression of the Igf2 gene. Nature 2000; 405: 482-485.

4 Chang J, Zhang B,Heath H, Galjart N, Wang X, Milbrandt J. Nicotinamide adenine dinucleotide (NAD)-regulated DNA methylation alters CCCTC-binding factor (CTCF)/cohesin binding and transcription at the BDNF locus. Proceedings of the National Academy of Sciences of the United States of America 2010; 107: 21836-21841.

5 Coward WR, Feghali-Bostwick CA, Jenkins G, Knox AJ, Pang L. A central role for G9a and EZH2 in the epigenetic silencing of cyclooxygenase-2 in idiopathic pulmonaryfibrosis. FASEB journal :

official publication of the Federation of American Societies for Experimental Biology 2014; 28: 3183-3196.

6 de Maat MF, van de Velde CJ, Umetani N, de Heer P, Putter H, van Hoesel AQ *et al*. Epigenetic silencing of cyclooxygenase-2 affects clinical outcome in gastric cancer. Journal of clinical oncology : official journal of the American Society of Clinical Oncology 2007; 25: 4887-4894.

7 Dekker J, Rippe K, Dekker M, Kleckner N. Capturing chromosome conformation. Science 2002; 295:1306-1311.

8 Dorsett D, Strom L. The ancient and evolving roles of cohesin in gene expression and DNA repair. Current biology : CB 2012; 22: R240-250.

9 Easwaran H, Johnstone SE, Van Neste L, Ohm J, Mosbruger T, Wang Q*et al*. A DNA hypermethylation module for the stem/progenitor cell signature of cancer. Genome research 2012; 22: 837-849.

10 Egloff S, Dienstbier M, Murphy S. Updating the RNA polymerase CTD code: adding gene-specific layers. Trends in genetics : TIG 2012; 28: 333-341.

11 Gilroy DW, Saunders MA, Sansores-Garcia L, Matijevic-Aleksic N, Wu KK. Cell cycle-dependent expression of cyclooxygenase-2 in human fibroblasts. FASEB journal : official publication of the Federation of American Societies for Experimental Biology 2001; 15:288-290.

12 Gomes NP, Espinosa JM. Gene-specific repression of the p53 target gene PUMA via intragenic CTCF-Cohesin binding. Genes &development 2010; 24: 1022-1034.

13 Hadjur S, Williams LM, Ryan NK, Cobb BS, Sexton T, Fraser P *et al*. Cohesins form chromosomal cis-interactions at the developmentally regulated IFNG locus. Nature 2009; 460: 410-413.

14 Hagege H, Klous P, Braem C, Splinter E, Dekker J, Cathala G*et al*. Quantitative analysis of chromosome conformation capture assays (3C-qPCR). Nature protocols 2007; 2: 1722-1733.

15 Heintzman ND, Stuart RK, Hon G, Fu Y, Ching CW, Hawkins RD *et al*. Distinct and predictive chromatin signatures of transcriptional promoters and enhancers in the human genome. Nature genetics 2007; 39: 311-318.

16 Hou C, Dale R, Dean A. Cell type specificity of chromatin organization mediated by CTCF and cohesin. Proceedings of the

National Academy of Sciences of the United States of America 2010; 107: 3651-3656.

17 Jin B, Robertson KD. DNA methyltransferases, DNA damage repair, and cancer. Advances in experimental medicine and biology 2013; 754: 3-29.

18 Kanduri C, Pant V, Loukinov D, Pugacheva E, Qi CF, Wolffe A *et al*. Functional association of CTCF with the insulator upstream of the H19 gene is parent of origin-specific and methylation-sensitive. Current biology : CB 2000; 10: 853-856.

19 Lai AY, Fatemi M, Dhasarathy A, Malone C, Sobol SE, Geigerman C *et al*. DNA methylation prevents CTCF-mediated silencing of the oncogene BCL6 in B cell lymphomas. The Journal of experimental medicine 2010;207: 1939-1950.

20 McGarvey KM, Van Neste L, Cope L, Ohm JE, Herman JG, Van Criekinge W *et al*. Defining a chromatin pattern that characterizes DNA-hypermethylated genes in colon cancer cells. Cancer research 2008; 68:5753-5759.

21 Murrell A, Heeson S, Reik W. Interaction between differentially methylated regions partitions the imprinted genes Igf2 and H19 into parent-specific chromatin loops. Nature genetics 2004; 36: 889-893.

22 Nitzsche A, Paszkowski-Rogacz M, Matarese F, Janssen-Megens EM, Hubner NC, Schulz H *et al*. RAD21 cooperates with pluripotency transcription factors in the maintenance of embryonic stem cell identity. PloS one 2011; 6: e19470.

23 Parelho V, Hadjur S, Spivakov M, Leleu M, Sauer S, Gregson HC *et al*. Cohesins functionally associate with CTCF on mammalian chromosome arms. Cell 2008; 132: 422-433.

24 Rhodes JM, Mc Ewan M, Horsfield JA. Gene regulation by cohesin in cancer: is the ring an unexpected party to proliferation? Molecular cancer research : MCR 2011; 9: 1587-1607.

25 Rizzo MT. Cyclooxygenase-2 in oncogenesis. Clinica chimica acta; international journal of clinical chemistry 2011; 412: 671-687.

26 Rodriguez C, Borgel J, Court F, Cathala G, Forne T, Piette J. CTCF is a DNA methylation-sensitive positive regulator of the INK/ARF locus. Biochemical and biophysical research communications 2010; 392: 129-134.

27 Rodriguez-Paredes M, Esteller M. Cancer epigenetics reaches mainstream oncology. Nature medicine2011; 17: 330-339.

28 Rubio ED, Reiss DJ, Welcsh PL, Disteche CM, Filippova GN, Baliga NS *et al*. CTCF physically links cohesin to chromatin. Proceedings of the National Academy of Sciences of the United States of America 2008; 105:8309-8314.

29 Schaaf CA, Kwak H, Koenig A, Misulovin Z, Gohara DW, Watson A *et al*. Genome-wide control of RNA polymerase II activity by cohesin. PLoS genetics 2013; 9: e1003382.

30 Song SH, Jong HS, Choi HH, Inoue H, Tanabe T, Kim NK *et al*. Transcriptional silencing of Cyclooxygenase-2 by hyper-methylation of the 5' CpG island in human gastric carcinoma cells. Cancer research 2001; 61:4628-4635.

31 Song SH, Hou C, Dean A. A positive role for NLI/Ldb1 in long-range beta-globin locus control region function. Molecular cell 2007; 28: 810-822.

32 Spilianakis CG, Lalioti MD, Town T, Lee GR, Flavell RA. Interchromosomal associations between alternatively expressed loci. Nature 2005; 435: 637-645.

33 Stadler MB, Murr R, Burger L, Ivanek R, Lienert F, Scholer A *et al*. DNA-binding factors shape the mouse methylome at distal regulatory regions. Nature 2011; 480: 490-495.

34 Tolhuis B, Palstra RJ, Splinter E, Grosveld F, de Laat W. Looping and interaction between hypersensitive sites in the active beta-globin locus. Molecular cell 2002; 10:1453-1465.

35 Toyota M, Shen L, Ohe-Toyota M, Hamilton SR, Sinicrope FA, Issa JP. Aberrant methylation of the Cyclooxygenase 2 CpG island in colorectal tumors. Cancer research 2000; 60:4044-4048.

36 Wang D, Dubois RN. Eicosanoids and cancer. Nature reviews Cancer 2010; 10: 181-193.

37 Wendt KS, Yoshida K, ItohT, Bando M, Koch B, Schirghuber E *et al*. Cohesin mediates transcriptional insulation by CCCTC-binding factor. Nature2008; 451: 796-801.

38 Yun J, Song SH, Park J, Kim HP, Yoon YK, Lee KH *et al*. Gene silencing of EREG mediated by DNA methylation and histone modification in human gastric cancers. Laboratory investigation; a journal of technical methods and pathology 2012; 92: 1033-1044.

# 국문초록

세포 내의 유전체는 다양한 3차 구조를 형성하는 것으로 알려져 있으며, 이러한 3차 구조는 다양한 유전자의 발현을 직접적으로 조절할 수 있는 것으로 알려져 있다. CCCTC-binding factor로 알려진 CTCF 단백질은 3차 구조를 형성하는데 있어 가장 잘 알려져 있는 구조 단백질로, 이들은 cohesin 단백질과 complex를 형성하여 서로 멀리 위치해 있는 유전자의 promoter와 enhancer를 가깝게 위치하게 함으로써 유전자 발현을 조절하는 것으로 알려져 있다. 하지만 이러한 구조 단백질에 의해 형성되는 유전체의 3차원적 구조가 암화 과정에 있어서 어떠한 역할을 수행하는지에 대한 연구는 부족한 실정이다.

CTCF 단백질은 CTCF 단백질 결합 부위 가까이에 위치한 CpG site의 methylation여부에 따라서 결합이 조절되는 것으로 알려져 있다. 따라서 암화 과정동안 암세포 특이적으로 나타나는 CpG island에서의 de novo methylation은 CTCF/cohesin을 매개로 하는 유전체의 3차 구조 형성에 있어 중요한 역할을 수행할 것으로 생각된다. 암화과정동안 CpG island de novo methylation에 의해 다양한 유전자의 발현이 저해되는 것으로 알려져 있으나, 이러한 에피지네틱 변이가 유전자의 전사를 어떻게 직접적으로 조절하는지에 대한 연구는 부족하다. 따라서 PTGS2라는 유전자를 대상으로 promoter CpG island de novo methylation에 의한 유전자 발현의 저해가 유전자 발현에 있어서 중요한 역할을 하는 것으로 알려진 CTCF/cohesin을 매개로 하는 유전체의 3차 구조 형성 변형에 의한 결과인지를 확인하고자 하였다.

PTGS2는 일부 위암세포주에서 promoter부위의 DNA methylation에 의해 저해되어 있는 것으로 알려져 있으며, CpG island 주변으로

CTCF와 cohesin binding site가 존재한다. 이를 토대로 실험을 진행하였으며, 실제로 PTGS2의 발현이 저해되어 있는 세포주 (SNU601)에서는 promoter부위에 methylation이 되어있고, CTCF/cohesin의 binding은 저해되어 있는 것을 확인하였다. 반대로 PTGS2의 발현이 높은 세포주 (SNU668)의 경우 promoter부위의 methylation이 확인되지 않고, CTCF/cohesin의 결합 역시 높게 나타나는 것을 확인하였다. Chromosome conformation capture (3C) assay 기법을 이용하여 이러한 CTCF/cohesin 결합의 차이는 해당 부위의 3차원적 구조와도 상관관계가 있음을 확인였다, 다시 말해, PTGS2의 발현이 높고 CTCF/cohesin결합이 많은 것으로 확인된 세포주 (SNU668)의 경우, 각각의 CTCF/cohesin결합 부위간의 거리가 그렇지 않은 세포주 (SNU601)보다 가까이 위치함을 확인하였다. 뿐만 아니라 demethylating agent로 알려진 5-Aza-CdR을 처리하여 SNU601에서 DNA methylation을 저해시킬 경우, promoter 부위의 DNA methylation이 감소하면서 유전자의 발현이 증가할 뿐만 아니라 해당 부위의 CTCF/cohesin의 binding 역시도 증가하는 것을 확인하였다. 이러한 CTCF/cohesin의 binding의 증가는 CTCF/cohesin 결합 부위간의 거리도 가깝게 만드는 것을 확인하였고, 이를 통해 DNA methylation이 CTCF/Cohesin 단백질의 결합을 조절할 수 있음을 증명하였고 이러한 결합 조절이 결과적으로는 유전체의 3차원적 구조를 조절하여 유전자 발현에 영향을 주는 것을 확인하였다. 마지막으로 SNU668에서 cohesin을 구성하는 단백질 중 하나인 Rad21을 저해시킴으로써, cohesin이 실제로 유전자의 발현과 PTGS2의 3차 구조를 직접적으로 조절할 수 있는지 확인하였다. 그 결과 Rad21 knockdown은 PTGS2의 유전자 발현을 저해시킬 뿐만 아니라 해당

부위의 3차원적 구조 역시도 조절함을 확인하였고, 이러한 3차원적 구조는 유전자 발현에 있어 중요한 역할을 수행하는 전사체가 해당 유전자에 형성되는데 있어 중요한 역할을 수행함을 증명하였다.

위와 같은 결과들을 토대로, 암화 과정 중에 나타나는 de novo CpG island methylation에 의한 유전자 발현 저해의 한 매커니즘으로 CTCF/cohesin을 매개로 하는 유전자의 3차원적 구조의 역할과 그 중요성을 증명하였다.

**주 요 어 ; 암, 후성유전학, DNA methylation, high-order chromatin structure**

**학 번 ; 2014-30804**